15th International Symposium on Practical Design of Ships and Other Floating Structures PRADS 2022

Dubrovnik, Croatia, October 9th – 13th 2022

Computational study on the potential transmission of COVID-19 virus on an Indonesian fishing vessel

Luofeng Huang[1,2,*], Wolter Hetharia[3], Andrea Grech La Rosa[2], Soegeng Riyadi[4], Dony Setyawan[4], I Ketut Aria Pria Utama[4] and Giles Thomas[2]

[1] School of Water, Energy and Environment, Cranfield University, UK
[2] Department of Mechanical Engineering, University College London, UK
[3] Department of Naval Architecture, University of Pattimura, Indonesia
[4] Department of Naval Architecture, Institut Teknologi Sepuluh Nopember, Indonesia

Abstract. During fishing operations, fishers often need to work in close proximity to each other on deck in a very limited space. This open-air working area can be subjected to various airflow conditions which might foster the airborne transmission of COVID-19 virus. To understand the risk of contagion in such a working environment and develop effective mitigation strategies to ensure the fishermen's safety, the present work establishes a computational model to analyse the virus' airborne transmission. Specifically, the work applies Computational Fluid Dynamic (CFD) to simulate various airflows occurring on an Indonesian fishing vessel, which is combined with Lagrangian particles that are used to model and track COVID-19 viruses. The concentration and coverage of COVID-19 viruses are analysed, considering the infected person working in different deck locations and under the influence of different vessel/wind speeds and directions. Subsequently, a set of guidelines including safe distance for the fishermen is suggested for each scenario.

Keywords*: COVID-19; Fishing Vessel; Virus; Airborne Transmission; Computational Fluid Dynamics; Particle modelling.*

1. Introduction

The global fishing industry has been facing COVID-19 issues, with a majority of vessels restricted from leaving port. Based on the authors' survey, in the Maluku provinces of Indonesia, only 30% - 40% of fishing vessels are currently operating. For the operating vessels, the catching process usually requires more than 10 crew members working side-by-side and the physical demands make it impractical to wear masks. Under these circumstances the crew's COVID-19 safety is of concern. There are approximately 2.2M fishers in Indonesia, owning more than 600,000 fishing vessels. The contemporary pandemic is causing enormous and increasing damage to the fishermen, thus urgent research is required [1].

In Indonesia, a primary type of fishing operation is Pole & Line (PL). Figure 1(a) presents the scenario of PL, where the crew fish in the bow area working in close proximity to take advantage of live bait thrown into the water. Figure 1(b) provides a corresponding drawing for this method.

It can be seen that the operation exposes the crew to COVID-19 risks, with the virus primarily transmitted via air and the infection can be induced through inhalation [2]. Especially, there can be particular airflow conditions which have been reported to foster the virus' airborne transmission [3]. Airflow may transmit viruses from an infected person to those nearby. Therefore, understanding the virus's movement and coverage in different airflow conditions is critical for developing effective mitigation strategies for the fishing industry.

Computational Fluid Dynamics (CFD) has demonstrated strong capabilities to simulate complex airflows, and the trace of virus particles in the flows may be tracked through a Lagrangian approach. This simulation technique has been successfully applied to COVID-19 transmission and mitigation, such as in a bus [4], in an aeroplane [5], inside a passenger vessel [3] and in a hospital [6]. The existing publications differ from the current work because they are all internal scenarios, while the crew working on a fishing vessel are generally in the open air. However, the CFD approach previously used to study the virus movements may be adapted to build a new model for the fishing scenario, which is presented here.

* Correspondence to: luofeng.huang@cranfield.ac.uk

(a) Photo of the operation

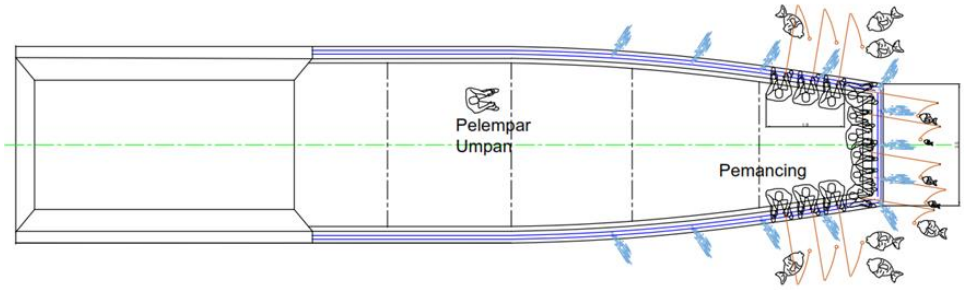

(b) Drawing of the operation

Figure 1: The PL fishing method

2. Computational modelling

2.1. Ship model and computational domain

A standard PL fishing vessel operating in Indonesia was selected as the research object of this paper, as shown in Figure 2. The ship has the following dimensions: length = 18 m, width = 4.2 m and height = 3.3 m. Based on a common working setup, it is assumed that 13 crew are working in the bow area, in which, 5 crew are in the bow and 4 crew are on each side. Typically there is a distance of 0.5 m between every two crew members on the deck. Accordingly, the computational geometry of the ship and the crew were built at full scale, as shown in Figure 3.

Figure 2: The fishing vessel used in this study, named “Yora 02” and operated by the company “CV Yora”

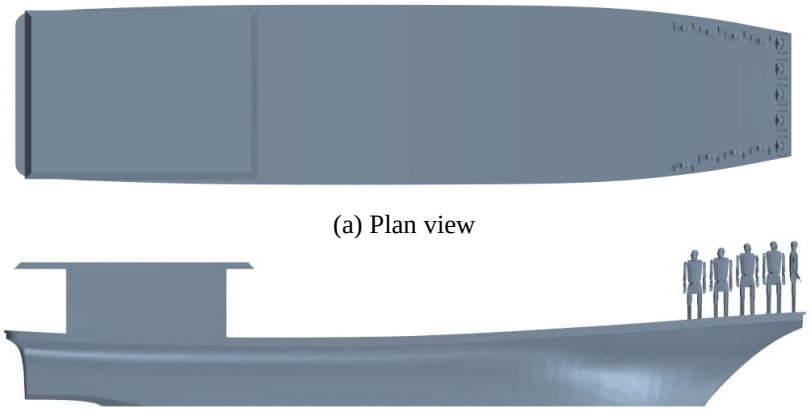

(a) Plan view

(b) Profile view

Figure 3: Computational geometry of the ship and crew

To perform CFD investigations, the geometry was imported into the STAR-CCM+ software. Then, a cuboid computational domain was established (60 m × 60 m × 6 m). There is at least one-ship-length domain on sides and behind the hull, which is large enough to avoid any boundary effect affecting the flow around the ship [7]. The bottom of the domain is set as a non-slip wall to mimic the water surface, considering a draught of 1 m. Other boundaries are mimicing open air, with the incoming wind boundary set as velocity inlet and the rests are set as pressure outlet. The domain was discretised into a mesh using hexahedral cells. A refined cell size (d) was used around the ship to obtain high-resolution results, while a relatively large grid size (10d) was applied for insignificant regions. The discretised domain is shown in Figure 4.

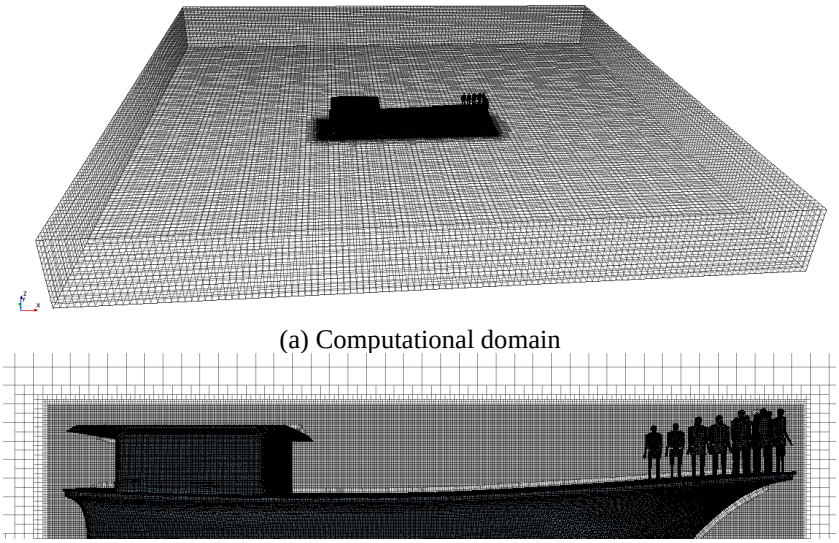

(a) Computational domain

(b) Close-up mesh view

Figure 4: Computational domain for CFD calculations

The ship was assumed to operate in airflow, and all grids were filled with air. No water was modelled in the current investigation to save computational cost, which is assumed to have no influence on the airflow in a calm-water condition. However, if waves were present, the heave, pitch and roll motions of the ship could influence the airflow.

A mesh sensitivity study was conducted with d = 0.12, 0.09, 0.06 m, resulting in 0.88, 1.92 and 6.09 million cells. The three sets of mesh were tested with a maximum Courant number of 1. The ship's air resistance in 15 knots headwind airflow is recorded, respectively 301 N, 271 N and 267 N. It can be seen that the resistance converges with the cell number increased, while the improvement d = 0.09 m and d = 0.06 m is not distinct. Therefore, the mesh with d = 0.09 m was selected to conduct the following analyses.

2.2. Governing equations

The governing equations of this work are the same as in [3], while applied to a different case here. The COVID-19 virus aerosols/droplets are modelled as Lagrangian particles. They are allowed to freely move in the Eulerian CFD mesh. Particles' movement is determined by their gravity (***G***) and a drag force from their surrounding airflow (***F_d***):

$$m\frac{\mathrm{d}\overline{\boldsymbol{V_P}}}{\mathrm{dt}} = \boldsymbol{G} + \boldsymbol{F_d} \tag{1}$$

where m denotes the particle's mass, $\overline{\boldsymbol{V_P}}$ is the particle's velocity, $\boldsymbol{G} = mg$ and g is set at 9.81 m/s^2. The fluid drag force is calculated through the Schiller-Naumann Correlation [8]:

$$\boldsymbol{F_d} = \frac{1}{2} C_d \rho_P A_P |V_s| \, V_s \tag{2}$$

where ρ_P is the particle density, A_P is the particle project area and V_s is the relative velocity between the particle and the air. C_d is an empirical coefficient calculated based on the particle's Reynolds number (Re_P), which is defined as follows.

$$C_d = \begin{cases} \frac{24}{Re_P}\left(1 + 0.15{Re_P}^{0.687}\right), & \text{if } Re_P \le 1000 \\ 0.44 \quad , & \text{if } Re_P > 1000 \end{cases} \tag{3}$$

Fluid properties in the CFD mesh are obtained by solving the standard Reynolds-Averaged Navier-Stokes (RANS) equations:

$$\nabla \cdot \overline{\mathbf{v}} = 0 \tag{4}$$

$$\frac{\partial(\rho\overline{\mathbf{v}})}{\partial t} + \nabla \cdot (\rho\overline{\mathbf{v}}\overline{\mathbf{v}}) = -\nabla\overline{p} + \nabla \cdot \left(\overline{\tau} - \rho\overline{\mathbf{v}'\mathbf{v}'}\right) + \rho g \tag{5}$$

where $\overline{\mathbf{v}}$ is the time-averaged velocity, $\mathbf{v}'$ is the velocity fluctuation, ρ is the fluid density (ρ_{air} = 1 kg/m^3), $\overline{p}$ denotes the time-averaged pressure, $\overline{\tau} = \mu[\nabla \mathrm{v} + (\nabla \mathrm{v})^{\mathrm{T}}]$ is the viscous stress term, and μ is the dynamic viscosity (μ_{air} = 1.48×10^{-5} N·s/m^2). Since the RANS equations have modelled fluid turbulence, the Shear Stress Transport (SST) $k-\omega$ model was adopted to close the equations [9,10].

For the present case, COVID-19 particles are microscopic and they can constantly perform stochastic motions. On the macro level, the stochastic motions reveal as the particles gradually diffuse. This behaviour is modelled by including the effect of instantaneous velocity fluctuations on the particle [11]:

$$\mathbf{v} = \overline{\mathbf{v}} + \mathbf{v}' \tag{6}$$

To be more specific, the applied fluid velocity in calculations is **v**, which is different from a usual RANS approach for macroscopic problems where $\overline{\mathbf{v}}$ is directly used to simplify the calculation, e.g. [12].

2.3. Study cases

The source of COVID-19 virus in this work is considered to be an infected person speaking. The airborne COVID-19 virus exists in a form of aerosols and droplets that can be generated by humans coughing, speaking, breathing, singing and sneezing [13]. Coughing and speaking are the most likely scenarios, as coughing is one of the primary COVID-19 symptoms whilst speaking is almost inevitable in daily contact and can output a significant amount of the virus. Chao et al. [14] measured the velocity, concentration and diameter of virus particles from coughing and speaking, as given in Table 1. They indicated that the duration of coughing is around 0.3 s, whilst speaking was considered to last 60 s. The viruses injected through coughing have a higher concentration and initial speed than those from speaking. However, the total quantity of viruses injected from speaking more than coughing because its duration is much longer. Therefore, the present work selected speaking over coughing as the virus source. A relevant work completed recently also demonstrated that speaking generally provides a higher COVID-19 risk than coughing [3].

Table 1: The details of virus import due to coughing and speaking [14].

Virus source	Coughing	Speaking
Injection duration	0.3 s, short event	60 s, long event
Inject speed	11.7 m/s	3.1 m/s
Particle diameter	13.5 μm	16 μm
Inject particle number	6950 per second	443 per second

There were two scenarios investigated in this work, headwind and tailwind conditions. For each scenario, three wind speeds were tested, 5 knots, 15 knots and 25 knots. The maximum of 25 knots was set according to on-site measurements. The wind may be considered as a relative flow, which is applicable to combined conditions with wind speed, vessel speed and relative heading angle. For each simulation, the infected person was assumed to be an upstream one, which is to ensure the maximal risk is studied.

3. Results and discussion

Following the CFD computation, Figures 5 and 6 present two examples for the airflows of a 25-knot headwind and tailwind, respectively. Figure 7 presents the virus trace in headwind conditions. It can be seen that the virus incurs a significant COVID-19 risk for the crew who are situated downstream from an infected-speaking person with a high concentration of virus particles. Comparing the results from different speed conditions, it is seen that high-velocity winds can help blow the viruses away and reduce the concentration. However, the risk is not eliminated even in the 25-knot case. It is also seen that a significant number of virus particles can be blown into the ship's superstructure. Therefore, the forward area should be cleaned frequently.

Figure 8 presents the virus trace in tailwind conditions. It can be seen that the ship superstructure can scatter the airflow, although the flow is not completely blocked; this is in line with Figure 6. Generally, the virus coverage and concentration are lower than for the headwind situation. Therefore, if the ship is not moving, placing the stern towards the wind could effectively reduce the COVID-19 risk. and the forward door and windows may be kept closed to prevent the virus from entering the cabin.

Combining the results of Figures 7 and 8, a safe distance may be suggested. According to the research of Vuorinen et al. [13], a COVID-19 infection can happen when at least 20 virus particles are inhaled. Taking an error-tolerant margin into consideration, this work defines a location with more than 10 virus particles as risky. Then, the virus trace's length that contains more than 10 viruses was measured, named Significant Trace Length (STL). A safe distance is suggested as the STL plus a 0.5 m distance that accounts for the crew's necessary motions during fishing. The calculated safe distance for each investigated case is reported in Table 2.

Table 2: Safe distance between crew

	Headwind	Tailwind
5 knots	2.5 m	1.5 m
15 knots	1.5 m	1 m
25 knots	1 m	0.5 m

Between 5-25 knots, the slower the wind, the larger STL is obtained. However, if the wind speed is zero, then there is no airflow to carry the virus, and the STL could be less than 0.5 m [3]. Therefore, future work will be conducted to check wind conditions between 0-5 knots to find out when the STL reaches its maximum. Additionally, the crosswind direction and oblique wind condition should also be investigated to obtain the corresponding STL.

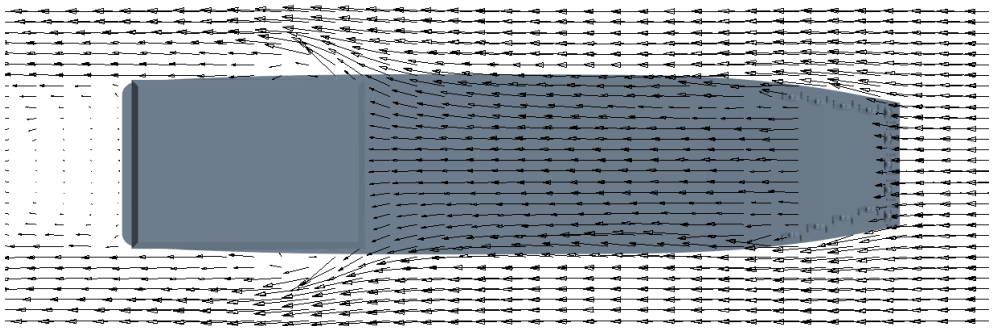

(a) Plan view

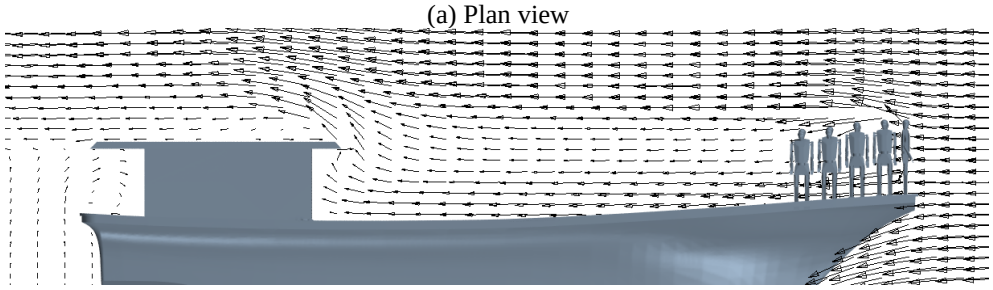

(b) Profile view

Figure 5: 25 knots headwind airflow

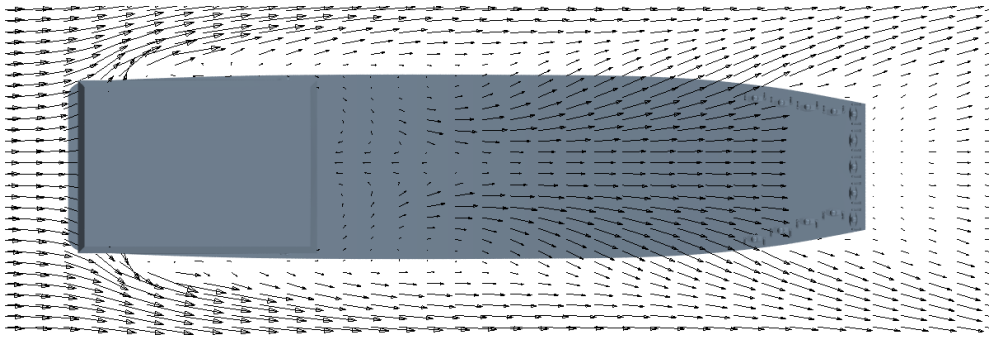

(a) Plan view

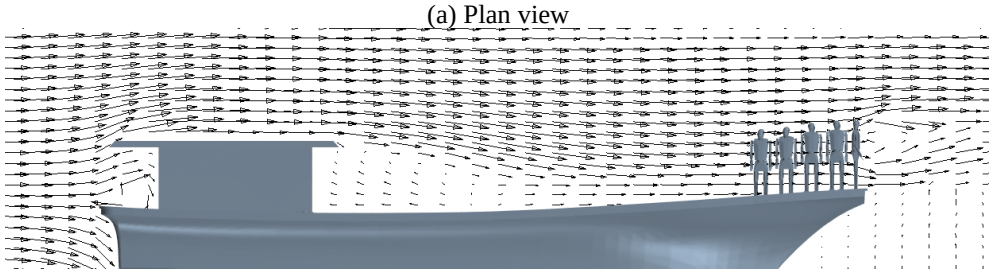

(b) Profile view

Figure 6: 25 knots tailwind airflow

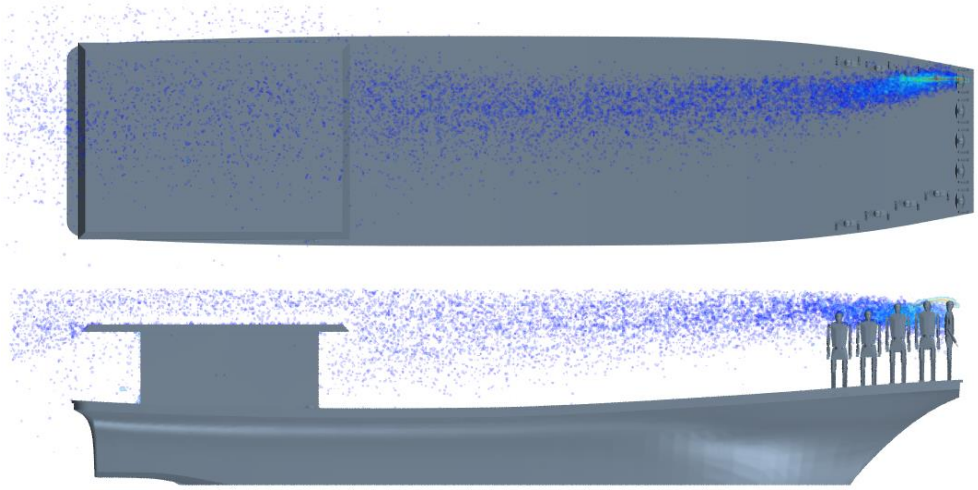

(a) 5 knots headwind airflow

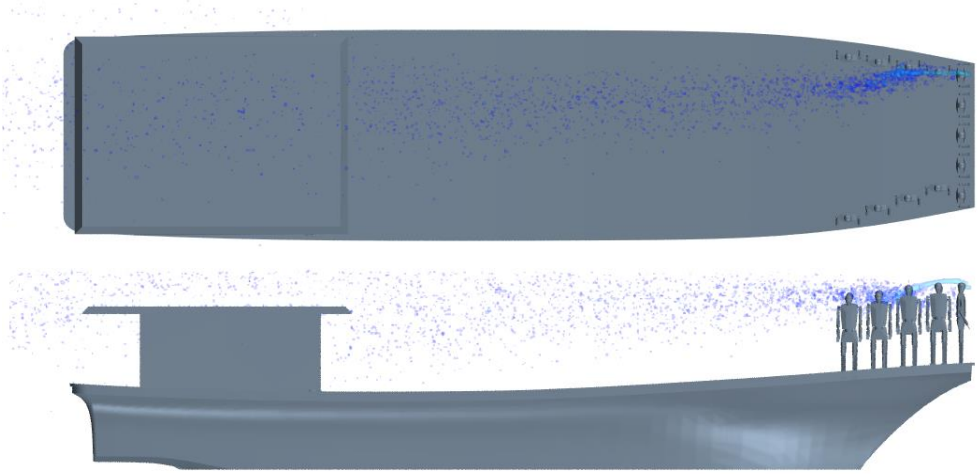

(b) 15 knots headwind airflow

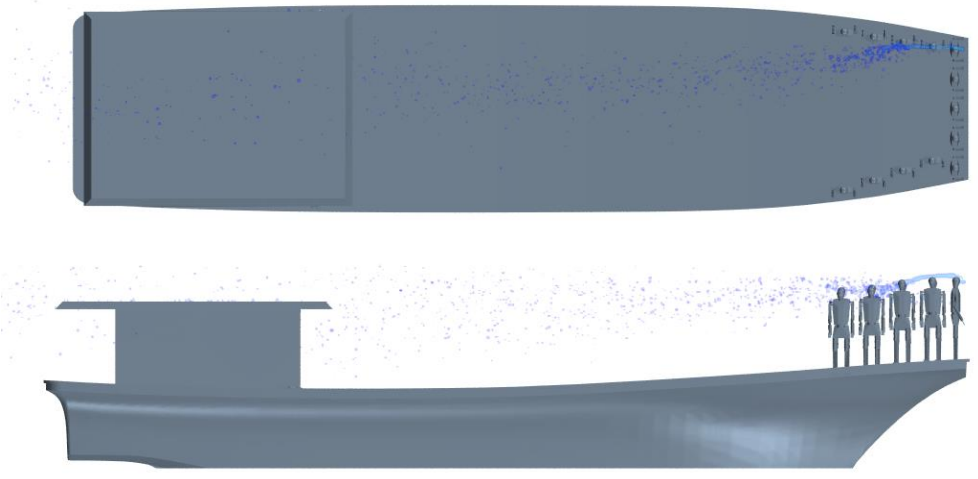

(c) 25 knots headwind airflow

Figure 7: Virus trace in headwind conditions

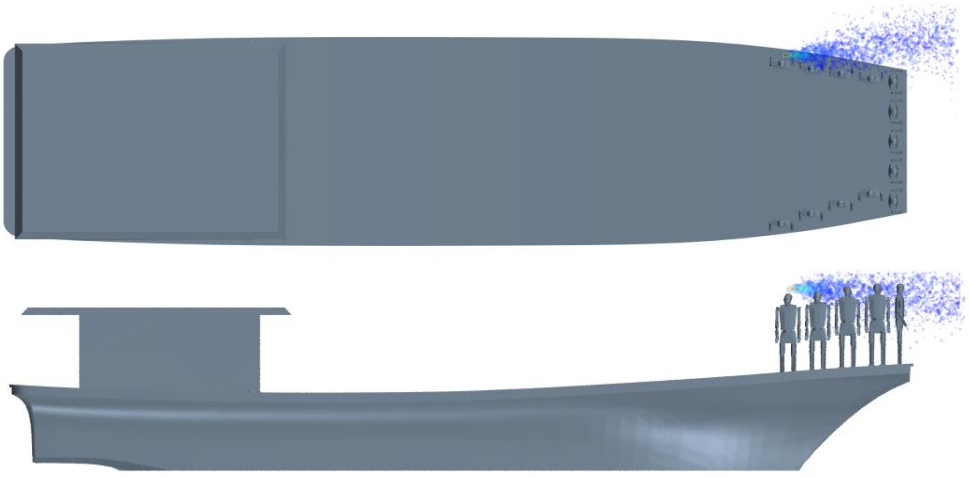

(a) 5 knots tailwind airflow

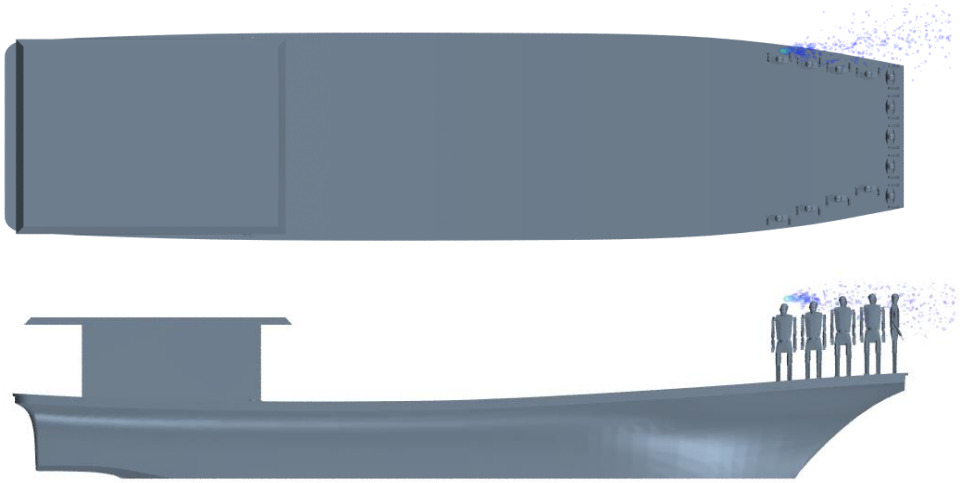

(b) 15 knots tailwind airflow

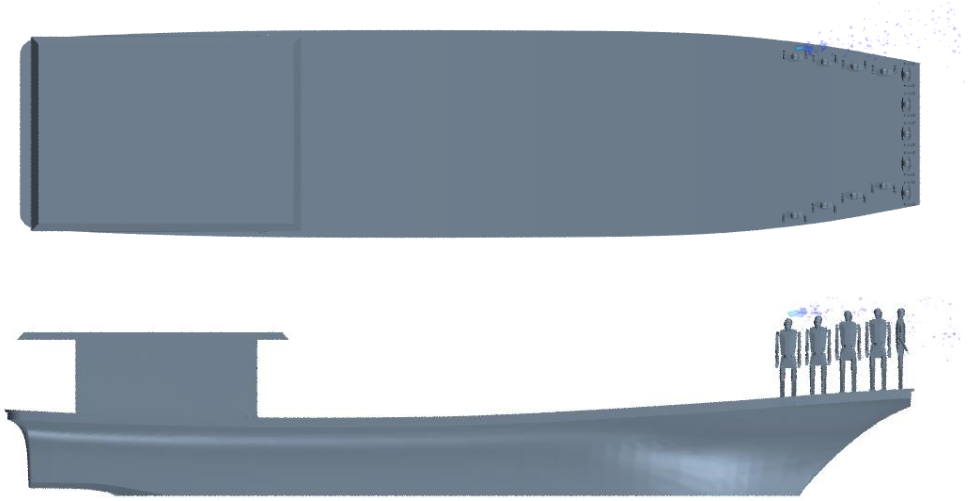

(c) 25 knots tailwind airflow

Figure 8: Virus trace in tailwind conditions

4. Conclusions

Fishing vessels in Indonesia and globally have been subject to a significant challenge from COVID-19. In order to recover their operations and aid the economic situation, this work has developed a computational model to analyse the COVID-19 risk during fishing operations. Headwind and tailwind conditions were investigated and it was found that the latter provide lower COVID-19 risk. Based on the risk-based intensity of virus particles in the air, a safe distance is suggested for each wind condition, which can be used as a guideline for the fishermen.

Acknowledgements

This work is part of a project that has received funding from the British Council under the Newton Institutional Links Grants - Ensuring the safety of Indonesian seafarers and fishers in the time of COVID-19 and beyond (agreement No. 623457938), in conjunction with the Indonesian Governmental Funding from the Ministry of Education, Culture, and Higher Education (agreement No. 1369/PKS/ITS/2022). The authors acknowledge the support of the CV Yora fishing company in sharing the studied vessel's geometry and details; the help of Mr Ibrahim Slamat is appreciated.

References

[1] G. Thomas, L. Huang, C. Ryan, I. Utama, S. Riyadi, D. Setyawan, W. Hetharia, Safer onboard environments for Indonesian seafarers and fishers in the time of COVID-19 and beyond, in: International Conference on Ship and Offshore Technology, The Royal Institution of Naval Architects (RINA), Surabaya, Indonesia, 2021.
[2] Y. Jin, H. Yang, W. Ji, W. Wu, S. Chen, W. Zhang, G. Duan, Virology, epidemiology, pathogenesis, and control of COVID-19, Viruses. 12 (2020) 372.
[3] L. Huang, S. Riyadi, I. Utama, M. Li, P. Sun, G. Thomas, COVID-19 transmission inside a small passenger vessel: Risks and mitigation, Ocean Engineering. 255 (2022) 111486. https://doi.org/10.1016/j.oceaneng.2022.111486.
[4] Z. Zhang, J. Capecelatro, K. Maki, On the utility of a well-mixed model for predicting disease transmission on an urban bus, AIP Advances. 11 (2021) 085229.
[5] K. Talaat, M. Abuhegazy, O.A. Mahfoze, O. Anderoglu, S.V. Poroseva, Simulation of aerosol transmission on a Boeing 737 airplane with intervention measures for COVID-19 mitigation, Physics of Fluids. 33 (2021) 033312.
[6] L. Guo, R. Torii, R. Epstein, J. Rubin, J.P. Reid, H. Li, A. Ducci, R. Balachandran, M.K. Tiwari, Y. Ventikos, L.B. Lovat, Using portable air purifiers to reduce airborne transmission of infectious respiratory viruses – a computational fluid dynamics study, MedRxiv. (2021) 2021.11.01.21265775. https://doi.org/10.1101/2021.11.01.21265775.
[7] ITTC, Guidelines: Practical Guidelines for Ship CFD Applications, ITTC Report. (2014).
[8] A.B. Liu, D. Mather, R.D. Reitz, Modeling the effects of drop drag and breakup on fuel sprays, SAE Transactions. (1993) 83–95.
[9] F. Menter, Zonal two equation kw turbulence models for aerodynamic flows, in: 23rd Fluid Dynamics, Plasmadynamics, and Lasers Conference, 1993: p. 2906.
[10] B. Pena, L. Huang, A review on the turbulence modelling strategy for ship hydrodynamic simulations, Ocean Engineering. 241 (2021) 110082.
[11] A.D. Gosman, E. Loannides, Aspects of computer simulation of liquid-fueled combustors, Journal of Energy. 7 (1983) 482–490.
[12] L. Huang, J. Tuhkuri, B. Igrec, M. Li, D. Stagonas, A. Toffoli, P. Cardiff, G. Thomas, Ship resistance when operating in floating ice floes: A combined CFD&DEM approach, Marine Structures. 74 (2020) 102817.
[13] V. Vuorinen, M. Aarnio, M. Alava, V. Alopaeus, N. Atanasova, M. Auvinen, N. Balasubramanian, H. Bordbar, P. Erästö, R. Grande, Modelling aerosol transport and virus exposure with numerical simulations in relation to SARS-CoV-2 transmission by inhalation indoors, Safety Science. 130 (2020) 104866.
[14] C.Y.H. Chao, M.P. Wan, L. Morawska, G.R. Johnson, Z.D. Ristovski, M. Hargreaves, K. Mengersen, S. Corbett, Y. Li, X. Xie, Characterization of expiration air jets and droplet size distributions immediately at the mouth opening, Journal of Aerosol Science. 40 (2009) 122–133.